

State of Health Estimation of Lithium-ion Battery Based on Early-stage Constant-voltage charging

Zhongbao Wei¹, Haokai Ruan¹, Xiaolei Bian², Hongwen He^{1*}

¹ National Engineering Laboratory for Electric Vehicles, School of Mechanical Engineering, Beijing Institute of Technology, China

² Department of Chemical Engineering, KTH-Royal Institute of Technology, Stockholm, Sweden

ABSTRACT

State of health (SOH) estimation is insightful for the lithium-ion battery (LIB) health management. This paper proposes a new set of health indicators (HIs) based on early-stage constant-voltage (CV) charging, which are easily available in practical vehicle applications. Particularly, a thorough analysis is performed over different CV-based HIs to obtain the informative ones with strong correlation against the SOH. A gaussian process regression (GPR) model is further employed to fusion the extracted HIs and to estimate the battery SOH. The proposed method is validated based on cycling experiments performed on the LiNiCoAlO₂ cells. Results suggest that the proposed method promises multifold benefits, including the high estimation accuracy, low requirement on the charging integrity, and the high robustness to cell inconsistency.

Keywords: lithium-ion battery, health indicators, state of health, constant voltage charging, gaussian process regression

1. INTRODUCTION

Lithium-ion battery (LIB) has been widely used as the onboard power source for electric vehicles (EVs) due to its high gravimetric/volumetric power density and low self charging. Within this horizon, a well-designed battery management system (BMS) is required to ensure the safety and longevity of LIB system. Especially, the estimation of state of health (SOH) is crucial for the BMS, which is insightful for the battery health management.

The SOH estimation has been a vast area of study giving rise to a variety of methods that can be categorized into model-based and data-based method.

For model-based method, SOH can be regarded as the state variable which are updated by adaptive filters [1-3]. However, such methods are sensitive to the model accuracy and limited by the high computing complexity.

The data-based methods extract informative health indicators (HIs) from the routine operation, and further use them to estimate the SOH. Machine learning methods like support vector machine (SVM) [4] and artificial neural network (ANN) [5] have been explored to capture the nonlinear mapping between HIs and SOH. Incremental capacity analysis (ICA) and differential voltage analysis (DVA) are two well-known data-based methods, where HIs extracted from the transformed charging profile are used for SOH estimation [6-8]. Albeit widely studied, the ICA and DVA depend on complete constant-current (CC) charging profiles, which is hardly available in reality, since LIBs are seldom full depleted before recharge.

Instead, the constant voltage (CV) charging profile is more easily available due to the drivers' tendency to fully charge their EVs whenever possible. Within this context, the time constant and charging duration of CV phase have been proved to be informative to estimate the SOH [9-11]. However, the time-consuming characteristic of CV phase, typically much longer than the CC phase but with much less charge recovered, leads to the lack of complete CV data, which restricts the extraction of CV-based HIs.

This paper aims to bridge aforementioned gap and proposes novel CV-based HIs to estimate the battery SOH. The main contributions of this paper are: (1) The novel HIs are extracted from 2000 seconds CV charging data by systematically analysis, which are easily available in practice. (2) A GPR model is employed to establish the deterministic relationship between the extracted CV-

based HIs and the SOH. Results show that the proposed method promises multiple merits of high estimation accuracy, high robustness to cell inconsistency and low requirement on the charging integrity.

2. HEALTH INDICATOR

2.1 Dataset description

Three NCA batteries from NASA Ames Prognostics Center of Excellence (PCoE), Moffett Field, CA, USA are employed, which are cycled under the constant current-constant voltage (CCCV) charging mode and CC discharging mode at room temperature. Discharging is carried out in CC mode at 2A until the terminal voltages of battery #5, #6 and #7 fall to 2.7V, 2.5V and 2.2V, respectively. Charging is carried out in CC mode at 1.5A until the battery voltage reaches 4.2V followed by a CV mode until the charge current drop down to 50mA. The battery nominal capacity is 2 Ah and the experiments are stopped when the battery reaches the end-of-life criteria, which is a 30% fade in nominal capacity.

2.2 Health indicators construction

Till now, no consensus definition of SOH has been proposed yet, and the ratio of the current capacity to nominal capacity is used to describe it in this paper:

$$SoH = Q_{cur} / Q_{nom} \quad (1)$$

where Q_{cur} is the current capacity and Q_{nom} is the nominal capacity.

2.2.1 Charging duration

Capacity degradation and CV charging curves at different cycles are shown in Fig. 1. It is observed that charging duration expands with the shrink of capacity, which is probably informative to refer SOH.

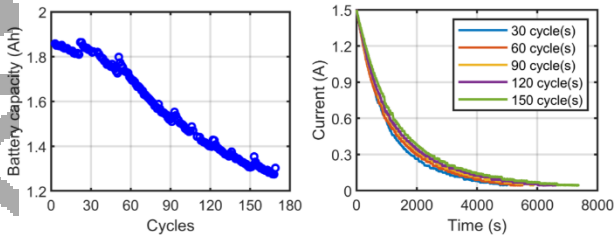


Fig. 1 Capacity degradation and CV charging curves at different cycles

In practical scenarios, only early-stage CV phase is easily available due to its time-consuming characteristic. Therefore, the regional charging duration experiencing a fixed current or capacity interval is proposed to estimate the SOH in this paper. The interval value is selected based on the specific application, and for CV charging data of NCA batteries, the current interval and capacity interval

are determined as 0.3A and 0.03Ah, respectively. To give a quantitative evaluation of the correlation between extracted HIs and SOH, correlation coefficients between the HIs and the battery capacity have been calculated by:

$$r = \frac{\sum_{i=1}^n (HI_i - \overline{HI})(Q_{max,i} - \overline{Q}_{max})}{\sqrt{\sum_{i=1}^n (HI_i - \overline{HI})^2} \sqrt{\sum_{i=1}^n (Q_{max,i} - \overline{Q}_{max})^2}} \quad (2)$$

The results of correlation analysis are shown in Fig. 2, where the CV current and CV capacity represent the terminal value of current interval and capacity interval, respectively. As shown in Fig. 2(a), it lacks a consistent conclusion about the selection of CV current region, as different cells exhibit distinct mode of correlation. In contrast, as shown in Fig. 2(b), the correlation coefficient tends to rise with the elevated capacity. It is concluded that the charging duration within regional capacity is more informative in terms of the suitability to infer the SOH. Three HIs are hence selected: (1) charging duration from 0.3-0.33Ah, (2) charging duration from 0.33-0.36Ah, (3) charging duration from 0.36-0.39Ah. It is worth noting that the regional capacity covering 0.3-0.39Ah corresponds to the CV charging time between around 1100 s and 2000 s, suggesting that only the early-stage CV data are used for extracting the HIs.

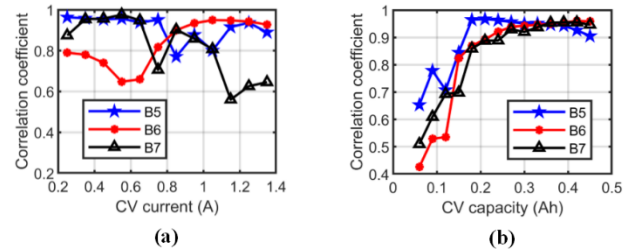


Fig. 2 Evaluation of different intervals: (a) current intervals and (b) capacity intervals

2.2.2 Model parameters

Theoretically, the dynamic characteristic of a battery can be accurately described by the equivalent circuit model (ECM) with infinite resistor-capacitor (RC) networks [12]. Herein the second-order RC model is employed to describe the long-short dual-scale dynamics of LIB. The architecture of the ECM is shown in Fig. 3.

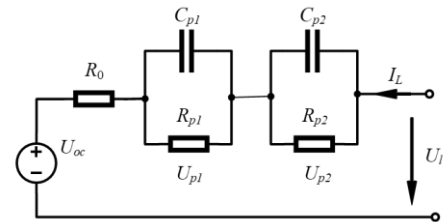


Fig.3 Second-order RC model of LIB

The electric behavior of the second order ECM can be expressed by follows:

$$\frac{dU_{p1}}{dt} = \frac{I_L(t)}{C_{p1}} - \frac{U_{p1}(t)}{C_{p1}R_{p1}} \quad (3)$$

$$\frac{dU_{p2}}{dt} = \frac{I_L(t)}{C_{p2}} - \frac{U_{p2}(t)}{C_{p2}R_{p2}} \quad (4)$$

$$U_L = R_0 I_L + U_{OC} + U_{p1} + U_{p2} \quad (5)$$

where I_L is the load current, R_{p1} and C_{p1} are the electrochemical polarization resistance and capacitance, R_{p2} and C_{p2} are the concentration polarization resistance and capacitance, R_0 is the internal resistance of the battery, and U_{OC} and U_L are open circuit voltage (OCV) and terminal voltage, respectively.

By means of Laplace transform, Eqs. (3)-(5) yield:

$$I_L(s) = \frac{(U_L(s) - U_{OC}(s))(sC_{p1}R_{p1} + 1)(sC_{p2}R_{p2} + 1)\eta}{\left[(sC_{p1}R_{p1} + 1)(sC_{p2}R_{p2} + 1)R_0 + (sC_{p2}R_{p2} + 1)R_{p1} + (sC_{p1}R_{p1} + 1)R_{p2} \right]} \quad (6)$$

Based on inverse Laplace transform, Eq. (6) can be expressed by:

$$I_L(t) = I_{L1}e^{-\frac{t}{\tau_{eq,1}}} + I_{L2}e^{-\frac{t}{\tau_{eq,2}}} + \frac{a}{c}(U_L - U_{OC}(t)) \quad (7)$$

where

$$a = R_0 R_{p1} R_{p2} C_{p1} C_{p2}$$

$$b = R_0 R_{p1} C_{p1} + R_0 R_{p2} C_{p2} + R_{p1} C_{p1} R_{p2} + R_{p2} C_{p2} R_{p1}$$

$$c = R_0 + R_{p1} + R_{p2}$$

$$\tau_{eq,1} = \left(b - \sqrt{b^2 - 4ac} \right) / 2a$$

$$\tau_{eq,2} = \left(b + \sqrt{b^2 - 4ac} \right) / 2a$$

where I_{L1} , I_{L2} , R_0 , C_{p1} , C_{p2} , R_{p1} and R_{p2} are the parameters to be identified, but U_{OC} is an unknown that needs timely update.

Converting Eq. (3) and Eq. (4) to the z-domain form and substituting them into Eq. (5), U_{OC} can be expressed as:

$$U_{OC}(z^{-1}) = U_L(z^{-1}) + \left[\frac{(1-\beta_1)R_{p1}z^{-1}}{1-\beta_1z^{-1}} + R_0 \right] I_L(z^{-1}) + \left[\frac{(1-\beta_2)R_{p2}z^{-1}}{1-\beta_2z^{-1}} + R_0 \right] I_L(z^{-1}) \quad (8)$$

where z is the discretization operator, $\beta_1 = \exp(-\Delta t_c / R_{p1}C_{p1})$, $\beta_2 = \exp(-\Delta t_c / R_{p2}C_{p2})$. By applying the discrete-transform, the following expression can be drawn:

$$U_{OC}(k) = \frac{\left[U_L(k) - (\beta_1 + \beta_2)U_L(k-1) + \beta_1\beta_2U_L(k-2) - R_0I_L(k) + (\beta_1 + \beta_2)R_0I_L(k-1) - \beta_1\beta_2R_0I_L(k-2) + U_m(k) \right]}{1 + \beta_1\beta_2 - (\beta_1 + \beta_2)} + \varepsilon(k) \quad (9)$$

where

$$U_m(k) = -\left[(1-\beta_1)R_{p1} + (1-\beta_2)R_{p2} \right] I_L(k-1) + \left[(1-\beta_1)\beta_2R_{p1} + (1-\beta_2)\beta_1R_{p2} \right] I_L(k-2) + \left\{ \beta_1\beta_2[U_{OC}(k-1) - U_{OC}(k-2)] + (\beta_1 + \beta_2 - \beta_1\beta_2)[U_{OC}(k-1) - U_{OC}(k)] \right\} \varepsilon(k) = \frac{\left\{ \beta_1\beta_2[U_{OC}(k-1) - U_{OC}(k-2)] + (\beta_1 + \beta_2 - \beta_1\beta_2)[U_{OC}(k-1) - U_{OC}(k)] \right\}}{1 + \beta_1\beta_2 - (\beta_1 + \beta_2)}$$

Noted that the error term $\varepsilon(k)$ is sufficiently small to be ignored. Hereby, the estimation of OCV is completed.

The OCV estimation and parameter identification are conducted in an iterative process, that is, the OCV is updated by Eq. (9) based on the identified parameters, which is in return feedback into Eq. (7) to identify the parameters. The algorithm terminates once the iteration number reaches the defined maximum threshold.

Taking battery #5 as an example, the correlation coefficients between the identified parameters and the battery capacity are shown in Fig. 4. It is observed that the values of R_0 and C_{p1} has relatively high correlation coefficients over 0.8 against the capacity. These two parameters are hence also employed as HIs to estimate SOH in this paper.

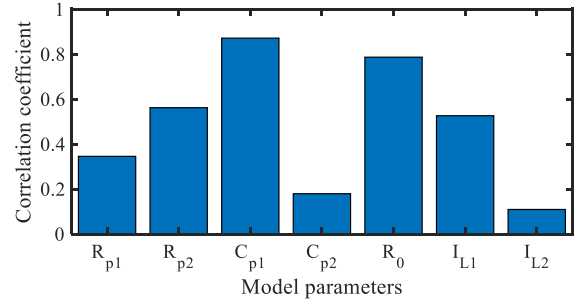


Fig. 4 Correlation between the extracted model parameters and the battery reference capacity

3. SOH ESTIMATION ALGORITHM

3.1 Gaussian process regression

The sophisticated electrochemical process leads to highly nonlinear characteristics of LIB, which challenges the accurate estimation of the battery SOH. Therefore, a GPR model is employed to fusion HIs belonging to different categories and to estimate the battery SOH.

Compared to ANN and SVM method, the GPR model shares a simpler structure, featured by a mean function and a covariance or kernel function:

$$m(x) = E(f(x)) \quad (10)$$

$$k(x, x') = E[(m(x) - f(x'))(m(x) - f(x')))] \quad (11)$$

where $m(x)$ is set to be zero for simplifying computing and the kernel function $k(x, x')$ describes the relevance degree between the training data set and the respective

inputs for model verification. The prior distribution of Gaussian process can be expressed as:

$$f(x) \sim N(0, k(x-x')) \quad (12)$$

Assuming that x and x' obey joint Gaussian distribution, then the predicted output y is derived by the joint prior distribution with the training output $f(x)$:

$$\begin{bmatrix} f(x) \\ y \end{bmatrix} \sim \begin{bmatrix} k(x, x) & k(x, x') \\ k(x, x')^T & k(x', x') \end{bmatrix} \quad (13)$$

Considering the diversity of extracted HIs in this paper, squared exponential kernel is exploited with automatic relevance determination:

$$k_{ARDSE}(HI, HI^*) = \sigma_f^2 \exp\left(-\frac{1}{2} \sum_{i=1}^n \frac{\|HI_i - HI_i^*\|^2}{\sigma_d^2}\right) \quad (14)$$

where σ_f is the parameter which tunes the amplitude of covariance and σ_d is the parameter which reflects the spread. In order to guarantee the performance of GPR, the parameters in the covariance function are optimized in the training process.

3.2 Framework of SOH estimation

A schematic diagram of the proposed method is shown in Fig. 5. Battery #5 is used to train the proposed method offline and online estimation is tested based on battery #6 and #7.

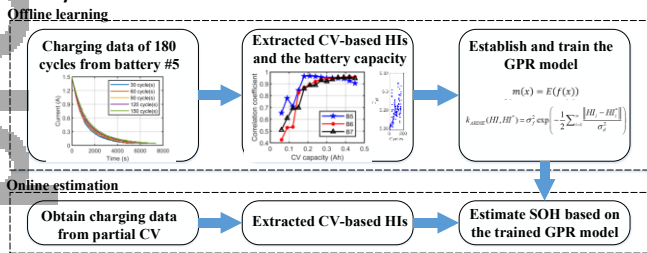


Fig. 5 Schematic diagram of the proposed method

4. RESULTS

4.1 SOH estimation

To evaluate the performance of the proposed method, the SOH estimation results based on battery #5, #6 and #7 are shown in Fig. 6 compared with existing SOH estimator based on the time constant. It is observed that the estimates match well with the benchmarked values. The absolute error is within the 5% bound except for a few outliers. It is noted that the proposed method trained by battery #5 performs accurately on the other two batteries, which validates its sufficient robustness to the cell inconsistency.

4.2 Comparative analysis

A comparative study is conducted for the proposed method and a reference method in the literature. The reference method extracts the CV time constant to infer the SOH [9]. Moreover, as the reference method uses the complete CV charging data, its counterpart using only the early 2000s data is also considered herein, for a fairer comparison with the proposed method.

The estimation results, measured by the mean absolute error (MAE), are listed in Table. 1 for a direct comparison. It is observed that the proposed method performs similarly with the reference method using complete CV charging data. Therefore, the proposed method actually shows an explicit superiority as it only needs the partial charging data in the early stage. Instead, if we perform the reference method under a partial charging scenario, it is found that the accuracy drops markedly to a level of low fidelity. It is thus concluded that the proposed method has a high robustness to the charging partialness, which appeals largely to the practical applications.

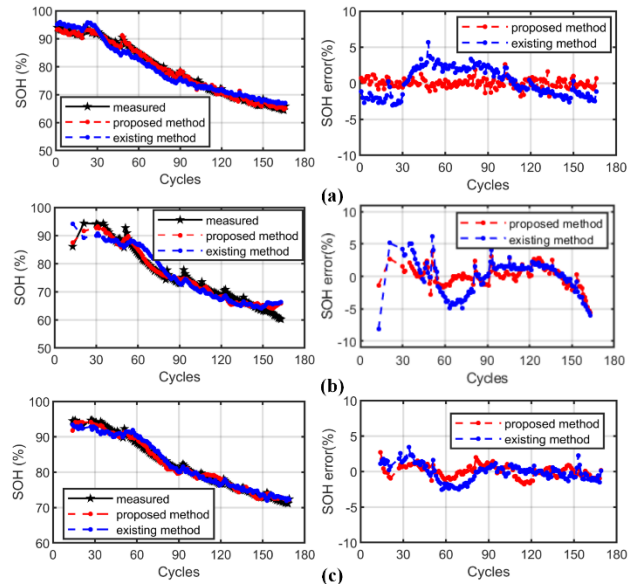


Fig. 6 SOH estimation results: (a) Battery #5, (b) battery #6 and (c) battery #7

Table. 1 MAEs of SOH estimation

method	B5	B6	B7
Proposed method	0.58%	1.56%	1.96%
Time constant with full CV charging data[9]	1.84%	2.14%	1.28%
Time constant with 2000s CV data	24.81%	16.5%	19.6%

5. CONCLUSIONS

A SOH estimation method based on CV feature extraction and fusion is proposed in this paper. A series of HIs are extracted based on partial CV charging data. A GPR model is further employed to combine different HIs and estimate the battery SOH. The proposed method has been validated on three NCA cells. The primary conclusions are summarized as follows:

(1) The charging duration for regional capacity and the identified dynamics parameters, extracted from the early-stage CV charging, proves to be highly informative for estimating the SOH.

(2) The proposed feature fusion-based method confines the SOH estimation error within the 5% error bound and shows merit of low requirement on the charging integrity compared to the conventional study.

ACKNOWLEDGEMENT

This work is supported by the National Key R&D Program of China (No. 2017YFB0103802).

REFERENCE

- [1] Wang Y, Chen Z. A framework for state-of-charge and remaining discharge time prediction using unscented particle filter. *Applied Energy*. 2020;260:114324.
- [2] Wei Z, Zhao J, Ji D, Tseng KJ. A multi-timescale estimator for battery state of charge and capacity dual estimation based on an online identified model. *Applied Energy*. 2017:S030626191730140X.
- [3] Wei Z, Meng S, Xiong B, Ji D, Tseng KJ. Enhanced online model identification and state of charge estimation for lithium-ion battery with a FBCRLS based observer. *Applied energy*. 2016;181:332-41.
- [4] You G-w, Park S, Oh D. Real-time state-of-health estimation for electric vehicle batteries: A data-driven approach. *Applied Energy*. 2016;176:92-103.
- [5] Wu Y, Xue Q, Shen J, Lei Z, Liu Y. State of Health Estimation for Lithium-ion Batteries Based on Healthy Features and Long Short-Term Memory. *IEEE Access*. 2020;PP:1-.
- [6] Li Y, Abdel-Monem M, Gopalakrishnan R, Berecibar M, Nanini-Maury E, Omar N, et al. A quick on-line state of health estimation method for Li-ion battery with incremental capacity curves processed by Gaussian filter. *Journal of Power Sources*. 2018;373:40-53.
- [7] He J, Wei Z, Bian X, Yan F. State-of-health estimation of lithium-ion batteries using incremental capacity analysis based on voltage-capacity model. *IEEE Transactions on Transportation Electrification*. 2020.
- [8] He J, Bian X, Liu L, Wei Z, Yan F. Comparative study of curve determination methods for incremental capacity analysis and state of health estimation of lithium-ion battery. *Journal of Energy Storage*. 2020;29:101400.
- [9] Wei J, Dong G, Chen Z. Remaining Useful Life Prediction and State of Health Diagnosis for Lithium-Ion Batteries Using Particle Filter and Support Vector Regression. *IEEE Transactions on Industrial Electronics*. 2018;65:5634-43.

[10] Yang J, Cai Y, Pan C, Mi C. A novel resistor-inductor network-based equivalent circuit model of lithium-ion batteries under constant-voltage charging condition. *Applied Energy*. 2019;254.

[11] Yun Z, Qin W. Remaining Useful Life Estimation of Lithium-Ion Batteries Based on Optimal Time Series Health Indicator. *IEEE Access*. 2020;8:55447-61.

[12] Yang J, Xia B, Huang W, Fu Y, Mi C. Online state-of-health estimation for lithium-ion batteries using constant-voltage charging current analysis. *Applied Energy*. 2018;212:1589-600.